CONTROL OF CARDIAC ALTERNANS IN A REALISTIC ELECTROMECHANICAL MODEL OF CARDIAC TISSUE

Azzam Hazim,[1] Youssef Belhamadia,[2] and Stevan Dubljevic[3]

[1]*Department of Biomedical Engineering, University of Alberta, Canada*
[2]*Department of Mathematics and Statistics, American University of Sharjah, UAE and Department of Biomedical Engineering, University of Alberta, Canada*
[3]*Deparment of Chemical and Materials Engineering, University of Alberta, Canada*

Electrical alternans is a physiological phenomenon manifested as beat-to-beat oscillation in cardiac action potential duration which has been shown to be a precursor to arrhythmias and sudden cardiac death. The majority of the existing control algorithms succeeded in suppressing alternans only in small pieces of cardiac cells. In this work, we will explore the feasibility of suppressing cardiac alternans in a realistic electromechanical model of relevantly sized cardiac tissue by using the mechanical perturbation strategy. The electrical activity is represented by the Luo-Rudy model, and the mechanical activity is represented by the Niederer-Hunter-Smith active contractile tension model and the Mooney-Rivlin passive elasticity model.

I. INTRODUCTION

Electrical alternans is a perturbation in the heart rhythm manifested as beat-to-beat oscillation (electric wave width alternation) of the cardiac Action Potential Duration (APD)[1]. Alternans have been shown to be a precursor to arrhythmias [2, 3] and sudden cardiac death (SCD), which is the most common cause of death in the industrialized world. APD alternans, is observed experimentally at high pacing rate so that beyond a critical pacing frequency the normally periodic response is replaced by a sequence of long and short APDs which is manifested as a variation in the width of action potential (see Fig. 1), the APD is the period of time during which the action potential exceeds the threshold value while the diastolic time interval (DI) in Fig.1 is defined as the period of time during which the action potential is below the given threshold value.

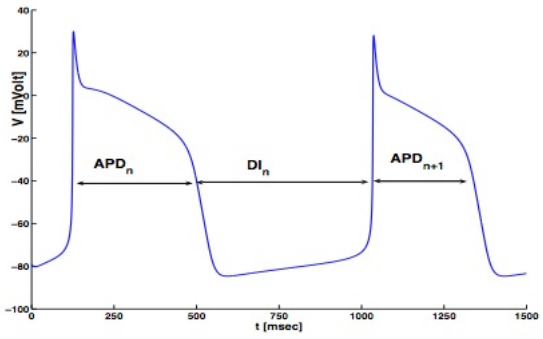

FIG. 1: Time evolution of transmembrane potential in the presence of alternans.

Many control algorithms have been developed to suppress alternans in cardiac tissue. However, most of these algorithms have only proved effectiveness for controlling electrical alternans in small tissues [4–7], up to 2.5 cm. In addition, to the authors' best knowledge, all the electric-based realization algorithms have not considered mechanical properties of cardiac tissue, despite the fact that mechanical deformation is shown to influence electrical activity of the heart tissue, and consequently the cardiac alternans. In fact, the propagation of action potentials in cardiac tissue initiate mechanical contraction via excitation-contraction coupling (ECC), while changes in tissue length due to contraction affect electrophysiological properties via mechanoelectrical feedback (MEF) [8, 9].

We [10] recently presented a novel mechanical perturbation algorithm to control alternans. The proposed algorithm succeeds to suppress cardiac alternans in relevantly sized cardiac tissues. However, in that study, we used a simple phenomenological model of cardiac excitation, and active tension was generated using an oversimplified isotropic active tension transient. Therefore, a more realistic electromechanical model of cardiac tissue should be used to investigate the control of alternans which is the goal of this study.

In this work, we will explore the feasibility of suppressing cardiac alternans in a realistic model by using the mechanical perturbation strategy. The electrical activity is represented by the Luo-Rudy [11] model, and the mechanical properties is described using the Mooney-Rivlin material response [10, 12]. The active tension that couples the electrophysiological model with the cardiac mechanics model is generated using the Niederer-Hunter-Smith [13] model which is the most advanced model, including all features contained in other models. Numerical simulations are presented to demonstrate that a model based on the mechanical and electrophysiological properties of cardiac tissue can be used to successfully suppress alternans in relevantly sized cardiac tissues.

II. MATHEMATICAL MODEL

We describe separately mathematical models of the cardiac mechanics and electrophysiology for an electromechanical model of cardiac tissue, and then describe a model that is used to couple these components via the generation of active tensions.

Cardiac Mechanics

To model deformation of the cardiac tissue, the mechanical analysis was based on finite deformation elasticity theory. The equilibrium equations as described in [10, 12], derived using Newton's laws of motion, are solved numerically to determine the mechanical deformation. The resulting equations are expressed as:

$$\frac{\partial}{\partial X_M}(S^{MN}F_{jN}) = 0 \tag{1}$$

where $F_{jN} = (\partial x_j/\partial X_M)$ is the deformation gradient tensor, X_M are the reference (undeformed) coordinates, x_i are the material (deformed) coordinates, S^{MN} is the second Piola-Kirchhoff stress tensor which is split into a passive and an active stress component [12] and is given by:

$$S^{MN} = \frac{1}{2}\left(\frac{\partial W}{\partial C_{MN}} + \frac{\partial W}{\partial C_{NM}}\right) + T_a C^{-1}_{MN}, \tag{2}$$

where $W(I_1, I_2)$ is the strain energy function, $C_{MN} = (\partial x_k/\partial X_M)(\partial x_k/\partial X_N)$ is the right Cauchy-Green deformation tensor, and T_a is the active tension generated by the electrical model. Mooney-Rivlin model [10, 12] is introduced to describe the mechanical properties of the tissue, and W for this model is given by:

$$W(I_1, I_2) = c_1(I_1 - 3) + c_2(I_2 - 3), \tag{3}$$

with $I_1(\boldsymbol{C}) = \mathrm{tr}(\boldsymbol{C})$ and $I_2(\boldsymbol{C}) = \frac{1}{2}(\mathrm{tr}(\boldsymbol{C}) - \mathrm{tr}(\boldsymbol{C}^2))$ are the first two principal invariants of $\boldsymbol{C}$, and $\mathrm{tr}(\boldsymbol{C})$ is the trace of $\boldsymbol{C}$, and c_1 and c_2 are material constants.

The direct influence of deformation on the electrophysiological properties is via the mechanoelectric feedback (MEF) which is provided by stretch-activated currents (SACs) as described in [14]:

$$I_{SAC} = G_s \frac{(\lambda_1 - 1)}{(\lambda_{max} - 1)}(V - E_s), \tag{4}$$

where G_s and E_s is the maximal conductance and reversal potential, respectively, and λ_1 is the fiber stretch, which is normalized by the maximal stretch (λ_{max}). The current I_{SAC} (4) is only present during stretch, and is added to the total ionic transmembrane currents generated by the LR1 model discussed in the cardiac electrophysiology.

Cardiac Electrophysiology

A monodomain model was used to represent cardiac electrophysiology, described by the following parabolic partial differential equation [15]:

$$C_m \frac{\partial V}{\partial t} = \frac{\partial}{\partial X_M}\left(D_{MN}\frac{\partial V}{\partial X_N}\right) - I_{ion} \tag{5}$$

where C_m is the membrane capacitance, V is the transmembrane voltage, t is time, D_{MN} is the conductivity tensor, and I_{ion} is the sum of the ionic transmembrane currents. We used Luo-Rudy-1 (LR1) [11] ionic model to represent electrophysiological properties of the heart. LR1 is a mammalian ventricular cell based model which incorporates interaction between depolarization and repolarization and accounts for the calcium dynamics in cardiac myocyte.

To take account the mechanical deformation of the tissue, neglected in this model, we modify (5) as described in [10, 12, 14] to give:

$$C_m \frac{\partial V}{\partial t} = \frac{\partial}{\partial X_M}\left(D_{MN}\sqrt{C}C^{-1}_{MN}\frac{\partial V}{\partial X_N}\right) - (I_{ion} + I_{SAC}) \tag{6}$$

Generation of Active Tension

We used Niederer-Hunter-Smith (NHS) [13] model for the generation of active tension (T_a) which is generated in response to electrical activation and coupled to nonlinear stress equilibrium equations. T_a in this model is dependent on quantities derived from both the cardiac mechanics model and the electrophysiological model. The general form of the equations of this model can be written as:

$$\frac{d\mathbf{w}}{dt} = \mathbf{g}(\mathbf{w}, \lambda_1, \frac{d\lambda_1}{dt}, [\mathrm{Ca}^{2+}]_\mathrm{i}), \tag{7}$$

$$\mathbf{w} = h^{-1}(T_a), \tag{8}$$

where $\mathbf{w}$ is a vector of internal state variables for the contraction model, $\mathbf{g}$ and h^{-1} are prescribed nonlinear functions. $[\mathrm{Ca}^{2+}]_\mathrm{i}$ is the intracellular concentration of Ca^{2+} ions generated by the LR1 model, and λ_1 is the fiber stretch calculated from the mechanics model.

III. CONTROL ALGORITHM

In this section, we describe the control algorithm developed to suppress alternans for the electromechanical model, described in the previous section, in 1D. The control scheme combines a pacer applied at the boundary, a spatially distributed, calcium based controller, and spatially distributed mechanical perturbation control.

First, the tissue is paced at the boundary at a critical pacing cycle length (PCL), named τ^*, such that the APD alternates. Under constant PCL, the amplitude of

alternans grows. The APD is measured from the instant when V crosses the threshold value during the depolarization phase, until the instant it falls below this value during the repolarization phase.

Boundary pacing control is realized by modulating the pacing interval based on the consecutive APDs at the pacing site, and is determined by the dynamic control scheme [5]:

$$T^n = \tau^* + \gamma(APD_n(\zeta = 0) - APD_{n-1}(\zeta = 0)) \quad (9)$$

T^n represents the amount of time between the n-th and $(n+1)$-th stimuli. Here γ is the feedback gain. This pacing control has the effect of suppressing cardiac alternans up to 1 cm from the pacing site. Beyond that region the instabilities grow along the tissue. To overcome this limitation in controllability, we combined it with a spatially distributed, calcium-based controller that modulates the intracellular Ca^{2+} concentration. This is motivated by recent studies [16, 17] that show that stretch-induced changes in intracellular calcium modify the electrical activity. The spatially distributed Ca^{2+}-controller is implemented in LR1 model as follows:

$$[Ca^{2+}]_i = -10^{-4} I_{si} + 0.07(10^{-4} - [Ca^{2+}]_i) + \alpha [Ca^{2+}]_{err}, \quad (10)$$

where $[Ca^{2+}]_{err} = [Ca^{2+}]_{pacer}(t - \tau_d) - [Ca^{2+}]_{i,control}$

It utilizes the difference between a stabilized delayed $[Ca^{2+}]$ at the pacing site and $[Ca^{2+}]_i$ over the length of area under spatially-distributed control. α is the controller gain, and τ_d is the time delay factor to account for the electrical wave propagation resistance along the tissue length. The controller acts after the electrical boundary feedback controller stabilizes a finite part of the tissue's length (≈ 1 cm).

A combination of the schemes ((9) and (10)) does not suppress alternans in the whole cable of the cardiac tissue cells, and more control effort is needed in order to control alternans in the electromechanical model, therefore, we added an error based feedback control algorithm implemented in NHS model that perturbs the tissue cardiac mechanics in a localized region. The spatially distributed mechanical perturbation control is implemented as follows:

$$\mathbf{w} = h^{-1}(T_a) + \beta e_n(\zeta) \quad (11)$$

where β is the controller gain, and $e_n(\zeta) = ATD_{\text{refs}}(\zeta) - ATD_n(\zeta)$. ATD is the width of active tension, it is measured from the instant when T_a crosses the threshold value on the wave front, until the instant it falls below this value on the wave back. This error is generated from the difference between the stabilized ATDs (ATD_{refs}), recorded before the onset of alternans, over the length of the area (3-4.5 cm) under spatially distributed control, and the ATDs at the n-th stimulus, over the same length of area.

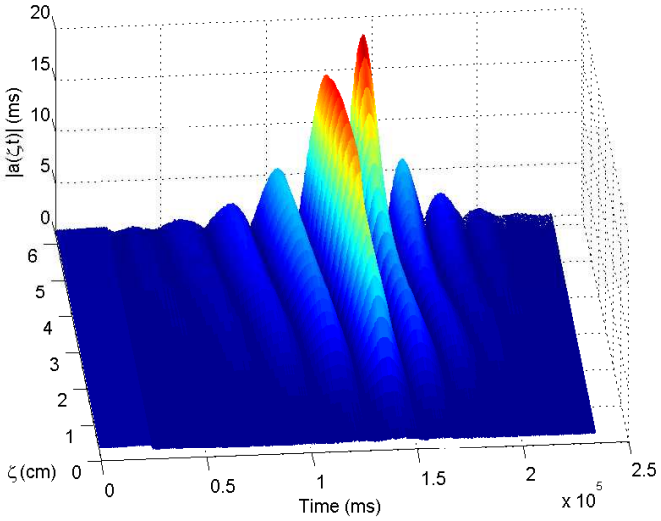

FIG. 2: Time evolution of the amplitude of alternans showing alternans suppression using mechanical perturbation and calcium based controller.

TABLE I: Parameter values for the mechanics model

$c_1 = 6$ kPa	$c_2 = 4$ kPa	$\lambda_{max} = 1.1$
$E_s = -20$mV	$G_s = 0.1\mu$S/μF	

IV. NUMERICAL RESULTS AND DISCUSSION

A one dimensional cardiac cable of the length $L = 6.25$ cm, fixed at the end points is considered. the diffusivity constant $C_m = 0.001\text{cm}^2/\text{ms}$ and the cell membrane capacitance $D = 1\mu\text{F/cm}^2$. All mechanics model parameters used in the simulation are given in Table I. For the given parameters, τ^* is found to be 307 ms. The controller gains γ, α, and β are chosen to be 0.3, 0.03, and 0.00002 respectively in the simulation. The excitation and active tension models were solved by explicit Euler scheme with step time $\Delta t = 0.05$ ms and step size $\Delta X = 0.025$ cm, and we determined the deformation mechanics of the tissue using finite difference scheme.

The amplitude of alternans, $a_n(\zeta)$, is defined as the difference between two consecutive APDs at a given point in space ζ:

$$a_n(\zeta) = (APD_n(\zeta) - APD_{n-1}(\zeta))(-1)^n \quad (12)$$

As shown in Fig. 2, the control signal of (10) and (11), applied at time = 150000 ms, which acts after the boundary pacing controller is applied at time = 10000 ms, successfully suppress alternans. The changes in T_a affect the mechanical deformation in (1), which then affects the transmembrane potential (6), through MEF.

The presence of electrical alternans induces, through the mechanism of ECC, an alternation in the heart muscle contractile activity. As shown in Fig. 3, the

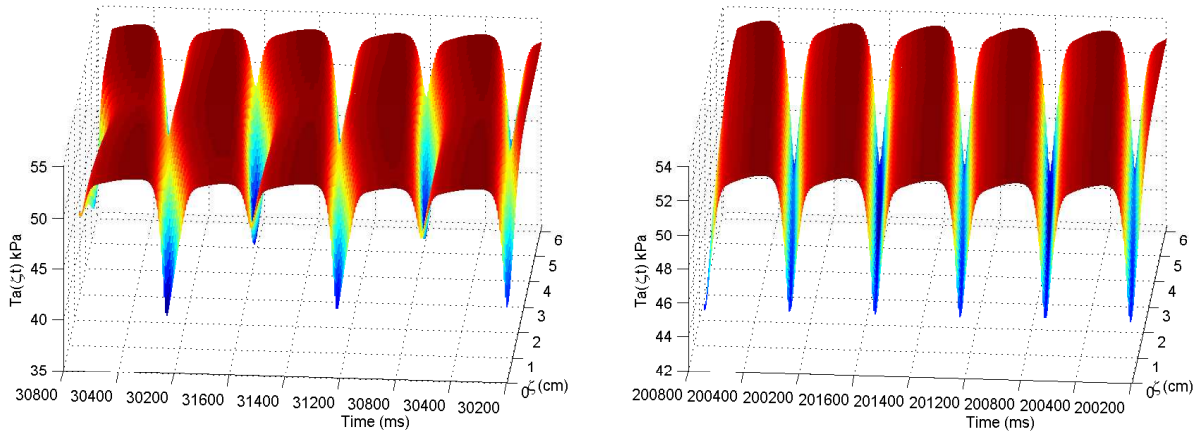

(a) (b)

FIG. 3: Time evolution of active tension T_a before (a), and after (b) the control is applied.

ATD width alternates when the control is not applied, Fig. 3a(a), and is suppressed, Fig. 3b(b), after the control is applied.

Although spatially distributed control is only applied over a localized region of the tissue (1.5 cm), it successfully suppress alternans. Thus, using a model based on the mechanical properties of cardiac tissue, it is clearly shown that spatially distributed mechanical perturbation control can be used to manipulate the electrical APD in order to suppress alternans along the whole cable of the cardiac tissue cells.

[1] G. R. Mines, "On dynamic equilibrium of the heart," *J. Physiol*, vol. 46, p. 349382, 1913.

[2] L. Makarov and V. Komoliatova, "Microvolt t-wave alternans during holter monitoring in children and adolescents," *ANN Noninvas Electro*, vol. 15, no. 2, pp. 138–144, 2010.

[3] S. M. Narayan, "T-wave alternans and human ventricular arrhythmias: What is the link?" *J Am Coll Cardiol*, vol. 49, no. 3, pp. 347–349, 2007.

[4] W.-J. Rappel, F. Fenton, and A. Karma, "Spatiotemporal control of wave instabilities in cardiac tissue," *Phys. Rev. Letts.*, vol. 83, no. 2, pp. 456–459, 1999.

[5] B. Echebarria and A. Karma, "Spatiotemporal control of cardiac alternans," *Phys Rev Lett*, vol. 88, p. 208101, 2002.

[6] D. J. Christini, M. L. Riccio, C. A. Culianu, J. J. Fox, A. Karma, and R. F. Gilmour Jr., "Control of electrical alternans in canine cardiac purkinje fibers," *Phys. Rev. Letts.*, vol. 96, no. 10, p. 104101, 2006.

[7] U. B. Kanu, S. Iravanian, R. F. Gilmour Jr., and D. J. Christini, "Control of action potential duration alternans in canine cardiac ventricular tissue," *IEEE Trans. Biomed. Eng.*, vol. 58, pp. 894–904, 2011.

[8] I. Kiseleva and *et al*, "Mechano-electric feedback after left ventricular infarction in rats," *Cardiovascular*, vol. 45, pp. 370–378, 2000.

[9] P. Kohl and U. E. Ravens, "Special issue on mechano-electric feedback and cardiac arrhythmias," *Progress in Biophysics and Molecular*, vol. 82, 2003.

[10] A. Hazim, Y. Belhamadia, and S. Dubljevic, "Control of cardiac alternans in an electromechanical model of cardiac tissue," *Computers in Biology and Medicine*, vol. 63, pp. 108–117, 2015.

[11] C. Luo and Y. Rudy, "A model of the ventricular cardiac action potential. depolarization, repolarization, and their interaction," *Circ Res*, vol. 68, pp. 1501–1526, 1991.

[12] M. P. Nash and A. V. Panfilov, "Electromechanical model of excitable tissue to study reentrant cardiac arrhythmias," *Prog Biophys Mol Bio*, vol. 85, pp. 501 – 522, 2004.

[13] S. A. Niederer, P. J. Hunter, and N. P. Smith, "A quantitative analysis of cardiac myocyte relaxation: a simulation study," *J Biophysics*, vol. 90, p. 16971722, 2006.

[14] R. Keldermann, M. Nash, H. Gelderblom, V. Wang, and A. Panfilov, "Electromechanical wavebreak in a model of the human left ventricle," *Am J Physiol Heart Circ Physiol*, vol. 299, pp. H134–H143, 2010.

[15] J. Keener and J. Sneyd, *mathematical physiology*. Springer-Verlag New York, 1998.

[16] D. M. Bers, "Cardaiac excitation-contraction coupling," *Nature*, vol. 415, pp. 198 – 205, 2002.

[17] S. C. Calaghan, A. Belus, and E. White, "Do stretch-induced changes in intracellular calcium modify the electrical activity of cardiac muscle?" *Prog Biophys Mol Biol*, vol. 82, pp. 81–95, 2003.